No. 40 May 1979

THE CALIBRATION OF A SCATTERANCE AND FLUORESCENCE METER

by

Eyvind Aas

INSTITUTT FOR GEOFYSIKK

UNIVERSITETET I OSLO

INSTITUTE REPORT SERIES

No. 40 May 1979

THE CALIBRATION OF A SCATTERANCE AND FLUORESCENCE METER

by

Eyvind Aas

ABSTRACT

Different methods of calibration are described and compared. New methods of scatterance calibration, which utilize the molecular scatterance of water, are presented.

CONTENTS

1. THEORY

1.1. Definitions

The symbols and definitions are whenever possible based on Standard Terminology on Optics of the Sea by IAPO Committee on Radiant Energy in the Sea, 1964 (quoted by JERLOV, 1976).

The volume scattering function $\beta(\theta)$ is defined as

$$\beta(\theta) = \frac{dI(\theta)}{E\, dv} \tag{1}$$

where dv is the scattering volume, E is the irradiance on dv, and dI is the intensity of the light scattered by dv in a direction θ from the incident beam. The intensity $dI(\theta)$ is defined as

$$dI(\theta) = \frac{d^2F(\theta)}{d\omega} \tag{2}$$

where $d^2F(\theta)$ is the light flux contained within the solid angle $d\omega$.. The irradiance E is defined as

$$E = \frac{dF_i}{dA} \tag{3}$$

where dF_i is the incident flux on the area dA normal to the beam. The volume scattering function may then be written

$$\beta(\theta) = \frac{d^2F(\theta)}{d\omega\, dv}\,\frac{dA}{dF_i} \tag{4}$$

The integral of β over all solid angles gives the scattering coefficient b:

$$b = \int_{4\pi} \beta\, d\omega = 2\pi \int_{0^\circ}^{180^\circ} \beta(\theta)\, \sin\theta d\theta \tag{5}$$

The attenuation coefficient c of a beam along the direction x is defined by

$$c = -\frac{dI}{dx}\,\frac{1}{I(x)} \tag{6}$$

The absorption coefficient a is the difference between the attenuation coefficient and the scattering

coefficient.

$$a = c-b \tag{7}$$

Some of the absorbed energy may be reemitted at longer wavelengths as fluorescent light.

A volume fluorescence function $\phi(\theta)$ is defined like β:

$$\phi(\theta,\lambda_x,\lambda_f) = \frac{dI(\theta,\lambda_f)}{E(\lambda_x)dv} = \frac{d^2F(\theta,\lambda_f)}{E(\lambda_x)dv\ d\omega} \tag{8}$$

where λ_x is the wavelength of the exciting light, and λ_f is the wavelength of the fluorescent light. The fluorescence coefficient f will similarly be

$$f(\lambda_x, \lambda_f) = \int_{4\pi} \phi(\theta,\lambda_x,\lambda_f)d\omega = 2\pi \int_0^{180^\circ} \phi(\theta,\lambda_x,\lambda_f)\sin\theta\, d\theta \tag{9}$$

Necessarily $f(\lambda_x,\lambda_f) < a(\lambda_x)$. An important tool in fluorescence studies is the quantum yield or quantum efficiency Q, which is defined as

$$Q = \frac{\text{number of quanta emitted (as fluorescence)}}{\text{number of quanta absorbed}} \tag{10}$$

Q will have values between 0 and 1. The relation between the number of quanta n at a wavelength λ and its energy e is

$$n = \frac{\lambda e}{ch} \tag{11}$$

where c is the velocity of light in vacuo and h is Planck's constant. Since the fluorescence appears as a continuous spectrum, eq.10 may be expressed as

$$Q = \frac{\int_{\frac{\lambda_f}{ch}} f_\lambda(\lambda_x,\lambda_f)d\lambda_f}{\frac{\lambda_x}{ch}\, a(\lambda_x)} = \int \frac{\lambda_f}{\lambda_x} \frac{f_\lambda(\lambda_x,\lambda_f)}{a(\lambda_x)}\, d\lambda_f \tag{12}$$

1.2. The angular dependence of molecular scatterance and fluorescence.

In Lord RAYLEIGH's 1918 model of light scatterance the molecules are allowed to have polarizabilities which depend upon their orientation in space. They are also assumed to be small compared with the wavelength, to be distributed at random in space, and to act like independent oscillators. The model then gives that the electric vector of the incident light will give rise to three independent dipole oscillators in the scattering volume, one "main" oscillator with its axis parallell to the electric vector, and two "sub"-oscillators of equal magnitude, perpendicular to each other and to the "main" oscillator.

If, for instance, the light is incident along the x axis with its electric vector parallel with the y axis, the main oscillator will be parallel with the y axis, and the sub-oscillators may be given directions parallel with the x and z axes. The scattering volume may be assumed to be at origo. Since the intensity from a dipole is proportional to $\cos^2\theta$, where θ is the angle between the direction of observation and the normal to the dipole, then the intensity component in the x-y plane, normal to a direction with deviation θ from the x axis, will be

$$I_{y\theta} = I_m\cos^2\theta + I_s\sin^2\theta = (I_m-I_s)\cos^2\theta + I_s \qquad (13)$$

where I_m and I_s are the intensity contributions from the main and the sub-oscillators in the x-y plane. The oscillator parallel with the z axis will give a vertical component at the same observation point in the x-y plane which is independent of θ:

$$I_{yz} = I_s \qquad (14)$$

If the electric vector of the incident light is turned so it becomes parallel with the z axis rather than with the y axis, then at the same observation point in the x-y plane we will have for the horizontal intensity component

$$I_{z\theta} = I_s\cos^2\theta + I_s\sin^2\theta = I_s \tag{15}$$

while the vertical component becomes

$$I_{zz} = I_m \tag{16}$$

When the incident light is unpolarized, we have for the horizontal component

$$I_\theta = I_{y\theta} + I_{z\theta} = (I_m - I_s)\cos^2\theta + 2I_s \tag{17}$$

and for the vertical component

$$I_z = I_{yz} + I_{zz} = I_s + I_m \tag{18}$$

The total intensity in a direction with angle θ from the incident ray, becomes

$$I(\theta) = I_\theta + I_z = 3I_s + I_m + (I_m - I_s)\cos^2\theta \tag{19}$$

It is convenient to introduce the depolarization ratio δ (CABANNES, 1920) defined by

$$\delta = \frac{I_y}{I_z} = \frac{I_\theta(90^\circ)}{I_z} = \frac{2I_s}{I_s + I_m} \tag{20}$$

Substitution of I_s in eq. 19 then gives

$$I(\theta) = \frac{2I_m}{2-\delta}\,(1+\delta+(1-\delta)\cos^2\theta) = I(90^\circ)\left(1+\frac{1-\delta}{1+\delta}\cos^2\theta\right) \tag{21}$$

Sometimes the depolarization ratio δ_p, due to incident light polarized in the z direction, is used.

$$\delta_p = \frac{I_{zy}}{I_{zz}} = \frac{I_{z\theta}(90^\circ)}{I_{zz}} = \frac{I_s}{I_m} = \frac{\delta}{2-\delta} \tag{22}$$

The relation of eq. 21 between intensity, angle and depolarization ratio is not only restricted to Rayleigh scattering, but is also valid for Raman scattering and fluorescence.

The Rayleigh scattered light, due to vibrations of the electrones, will have the same wavelength as the incident light, and the scattering process takes place during the period of the light wave, which is of order 10^{-15} seconds.

If the nuclei of the atoms in the molecules were fixed in position, this would be the only molecular scattering observed. However, since the nuclei are capable of vibration and rotation, they can, during the scattering process abstract a certain quantum of energy from the incident light quanta and convert it to vibrational energy. The Raman scattered light quanta which have lost this quantum of energy, will then differ from the Rayleigh scattered quanta by having a frequency which is decreased by a certain amount. The process may also be reversed, so that a higher frequency results, but the intensity of this Raman line is weaker than the former (PARKER, 1968).

Apart from the amount of light which is scattered from the beam, some may also be absorbed. The absorbed energy will excite the electrons to higher energy levels, and some may later be converted to thermal or chemical energy, while some parts may be reemitted as fluorescent light. The emitted light quantum cannot have a higher energy than the absorbed one, and the fluorescent light will then have lower frequencies than the incident light. Contrary to the Raman scattering, the wavelengths of the fluorescence spectrum are independent of the wavelength of the absorbed incident light. Another important difference is that while Rayleigh and Raman scattering take place during ca. 10^{-15} seconds, the emission of fluorescence is much slower, of order 10^{-9} seconds or more. (When the lifetime of the emission is 10^{-4} seconds or greater, the process may be termed phosphorescence (PARKER, 1968)). During this time the emitting molecule may rotate due to brownian movements, and the resultant light distribution is likely to be more isotropic, that is δ will become closer to 1.

$I(\theta)$ in eq. 21 is identical with the scattered intensity dI in eq. 1. Eq. 21 then gives

$$\beta(\theta) = \beta(90^{\circ})(1 + \frac{1-\delta}{1+\delta} \cos^2\theta) \tag{23}$$

and similar relations may be obtained for the Raman scatterance and the fluorescence.

The integral of eq. 23 is:

$$b = 4\pi\, \beta(90^{\circ})(1+ \frac{1}{3} \frac{1-\delta}{1+\delta}) \tag{24}$$

1.3. Error estimates

Since different methods with different accuracies are used, I have found it convenient to estimate the standard deviation of the physical quantities whenever possible. If y is a function of $x_1, x_2, x_3 \ldots$, the standard deviation s_y of y is computed from

$$s_y = \sqrt{(\frac{\delta y}{\delta x_1} s_{x_1})^2 + (\frac{\delta y}{\delta x_2} s_{x_2})^2 + \ldots\ldots\ldots} \tag{25}$$

When a sufficient number N of observations of x exists, so that a reliable mean value $\bar{x} = (\Sigma x)/N$ can be calculated, then the standard deviation of $\bar{x}$ is employed

$$s_{\bar{x}} = \sqrt{\frac{\Sigma(\bar{x}-x)^2}{N(N-1)}} \tag{26}$$

In other cases s_x may be estimated from the precision of the measurement, or from the variation of values given in the literature.

2. THE INSTRUMENT

Similar instruments have been described earlier by JERLOV (1953) and HØJERSLEV (1971). The present instrument was constructed by Mr. KJELL NYGÅRD (Institute of Physical Oceanography, University of Copenhagen). It is a laboratory meter, designed for work at sea, and consists of a water sample section between a lamp section and a photomultiplier section (Fig. 1). When the collimated light beam from the lamp penetrates the water sample, particles as well as water molecules will scatter the light, and dissolved organic matter may fluoresce. The photomultiplier and the connected amplifier produce a signal which depends on the intensity and wavelength of the received light. The signal from a bottle of compact plexi-glass is used as reference.

2.1. The lamp section

The lamp is a Philips High Pressure Mercury Quartz Burner HPK 125 W. The light is collimated by a lens, and passes through a filter disk and a glass window into the sample section. The irradiance spectrum of the lamp, based on data from the manufacturer and measurements inside the sample section, is shown in Fig. 2. The spectrum consists of several strong lines, together with a weaker continuous spectrum. In Fig. 2 the lines have been drawn as parts of the continuous spectrum, with a width of 10 nm. With the applied filter combinations the contributions to the signals from the continuous spectrum will be of order 10% of the contributions from the lines. The irradiance was measured by means of a selenium irradiance meter and a "Lambda" quanta meter, both provided with different filters. The results coincided well.

The entrance filter disk has two interference filters, one for the Hg line at 366 nm, and one for the line at 546 nm. The transmittance of the first filter, termed UV, is shown in Fig. 3. The disk also has an open hole as well

as a position for no transmittance.

The light is observed to be unpolarized.

2.2. The photomultiplier section

The photomultiplier "views" the water sample through a pinhole, a filter, a lens, and a glass window (Fig. 1). The filters, which are inserted in the filter disk, are the Schott & Genossen glass filters:

B12, 2 mm thick, which together with the entrance UV select the line at 366 nm. (The UV filter may also be used alone for this purpose, but fluorescence may then contribute to the signal). When the B12 filter is used alone, with no entrance filter, the lines at 366, 406 and 436 nm are transmitted with gravity center at 406 nm.

V9, 4 mm, which selects the line at 546 nm.

O2, 2 mm, which selects the line at 578 nm.

R1, 2 mm, which transmit the weak continuous spectrum in the red part. The combination of filter and photomultiplier gives a gravity center about 630 nm.

The filter disk also has a combination of one Wratten filter 2B and two 47B, which together with the entrance UV filter is used to select out the Raman line of pure water at 418 nm, scattered by light at 366 nm. The Wratten combination is termed BR. It may also be used alone to select the line at 436 nm. The transmittance of the different filters are presented in Fig. 3.

The photomultiplier is a Dumont 6467 tube. The sensitivity curve, given by the manufacturer, was adjusted by observations obtained by replacing the tube and pinhole with instruments of calibrated spectral sensitivity. The table below illustrates the agreement between the different measurements. The resultant sensitivity curve is shown in Fig. 3.

	Spectral sensitivity of the instrument, relative to 436 nm.				
Wavelength in nm	Dumont data	Relative to Lambda meter	Relative to EEL sel.cell	Relative to B.Lange sel.cell	Applied values
366	0.71		0.89±0.03	088±0.02	0.89±0.03
436	1	1	1	1	1
546	0.59	0.76±0.03	0.73±0.03		0.75±0.03
576	0.36	0.50±0.02	0.47±0.01		0.48±0.02
630	0.04	0.054±0.005	0.055±0.001		0.055±0.005

The amplified signals from the photomultiplier may normally be recorded within a range of 5 decades. However, by varying the high voltage over the photomultiplier, this range may be extended.

2.3. The water sample section

The water samples are kept in selected 100 ml glass bottles with a diameter of 5 cm from Jenaer Glaswerk Schott & Genossen. In order to minimize reflection and refraction at the bottle surface and the cell walls, the space between the bottle and the walls is filled with water.

The effect of bottles on the signal were checked by measuring first the signals from the sample cell filled with water, but without any bottle, and then the signals from the bottle, filled with the same water. The bottles were also turned to see if deviations in glass thickness or curvature would influence the signal. No effects could be found within the accuracy of the measurements. Any effect is then at least less than 5% of the signal from the plexi-glass standard.

The plexi-glass standard, however, contains optical axes which increase the signal with 6 to 8% from the minimum value, when turned (Fig. 4). As a practical rule the standard has been used with the direction for minimum

signal. The plexi-glass cylinder has a diameter of 5.4 cm, and its refractive index and attenuation coefficient are shown in Fig. 5. It is seen that the attenuation coefficient at 366 nm is 0.02 pr.cm, while at 436 nm it is 0.006 pr.cm. Some part of the attenuated light is absorbed, and some part of this again produces fluorescence. The fluorescence will increase the signals at the longer wavelengths. For instance, measurements with the regular R1 filter is about 25% higher when an extra R1 filter is added between the plexi-glass standard and the photomultiplier, than if it is added between the standard and the lamp. The table below gives the influence of fluorescent light on the plexi-glass standard at 45° angle at this instrument.

	Contribution in per cent of the total signal		
	V9	O2	R1
From the line at 366 nm	3.8±0.5	3.0±0.7	18.5±0.5
From the lines at 406 and 436 nm	3.3±1.3	1.4±0.5	6.5±0.5
Sum	7±2	4±1	25±1

Thus the signals with filters V9, O2 and R1, are not only due to the scattering properties of the standard at 546, 578 and 630 nm, but also due to its fluorescence properties at shorter wavelengths. However, as long as the spectrum of the mercury lamp remains fairly constant, this creates no problem.

While the thin walls in the sample bottles produced no observable refraction effects, the compact plexi-glass cylinder has a considerable "lens" effect. Its chromatic aberration influences the amount of light of different wavelengths which passes through the lens and pinhole to the photomultiplier. The signals consequently depend also on the optical geometry of the standard and the instrument, and not only on its internal optical properties. The

optical properties attributed to the standard here, can then not be transferred to other optical systems. The great advantage of the plexi-glass standard, however, is that it gives a reliable reference with signals of the same order as those of sea water.

3. THE CALIBRATION PROBLEM

In an ideal scatterance meter one might determine $d\omega$, dv and dA from the geometrical and optical dimensions of the instrument, and by measuring dF_i on dA and d^2F within $d\omega$, β might then be calculated from eq. 4. However, in many scatterance meters it is not possible to measure the incident flux with the same light detector as that applied to the scattered flux. Even if possible, it may be inconvenient that the ratio between the two fluxes is of order 10^6 or greater. It is easier if some sort of substandard may be used.

In Chapter 4.1 (Method 1) the diffusing properties of magnesium oxide is applied together with estimates of the finite quantities ω, v and A in order to calibrate the scatterance of the standard.

A problem which arises by the use of the finite quantities above is whether the irradiance E is constant over A and whether the instrumental sensitivity of scattered flux is constant within ω. An ingenious method which solves this problem is mentioned by BLAKER et al. (1949). A similar method is described in detail by PRITCHARD and ELLIOTT (1960). Modified versions are given by TYLER (1963) and FRY (1974). Method 2 (Chapter 4.2) is an application of these principles.

For non-absorbing particles, the particle attenuation coefficient c_p will be equal to the particle scattering coefficient b_p. If the particles also are so small that they scatter light according to Rayleigh's equation, the instrument is easily calibrated when c and β are measured for the solvent and the solution (WEBER and TEALE, 1957). DEZELIC and KRATOHVIL (1960) have found that Ludox

colloidal silica, with mean diameter of 17-19 nm, behave practically as Rayleigh scatterers. However, such a method has not been applied here.

EASTMAN (1967) uses the result of DEZELIC and KRATOHVIL to calibrate a fluorometer and to find the fluorescence quantum yield of quinine sulfate. This procedure may also be reversed, so that the known fluorescence of quinine sulfate is used to calibrate the scatterance meter. Chapter 4.3 describes such a method (Method 3).

Pure liquids with known scatterance may be used as calibration standards. Some values are given in the table below. n is the index of refraction relative to air, b is calculated from eq. 24.

	λ nm	Carbon disulfide CS_2	Benzene C_6H_6	Carbon tetrachloride CCl_4	Methanol CH_4O	Water H_2O
$\beta(90^\circ)$ $(10^{-4}m^{-1})$	436	274	45.6	14.8	6.55	2.32
	546	84.6	15.8	5.53	2.42	.865
	633	42.6	8.5	2.95	1.42	.490
δ	436	.667	.433	.052	.059	.087
	546	.656	.424	.049	.051	.076
	633	.650	.432	.042	.050	.076
n	436	1.67	1.52	1.47	1.33	1.34
	546	1.63	1.50	1.46	1.33	1.33
	633	1.62	1.50	1.46	1.33	1.33
b $(10^{-3}m^{-1})$	436	367	64.9	24.2	10.7	3.73
	546	114	22.5	9.05	3.96	1.40
	633	57.3	12.1	4.84	2.32	.792

Sources: 436 and 546 nm: COHEN and EISENBERG (1965),
633 nm: PIKE et al. (1975).

While carbon disulfide has a scatterance which is about 100 times greater than that of water, it also has a much greater refractive index (in fact higher than that of the plexi-glass standard), and this will besides "lens effects"

also produce a scattering volume and a solid angle (eq. 4) which are different from the corresponding ones in water.

I think it is more safe to calibrate with water, since the instrument is used for water scatterance measurements. The disadvantage with water, on the other hand, is that its scatterance is relatively weak, and consequently very sensitive to impurities. It then becomes difficult to obtain optically "pure" water. Methods which still utilize the Rayleigh scatterance, although the waters are impure, are described in Chapter 4.4 to 4.6 (Methods 4 to 6).

4. SCATTERANCE CALIBRATION

4.1. Method 1. The fixed MgO disk

4.1.1. The diffusing properties of MgO

When a disk is smoked over burning magnesium ribbon, a matt white surface of magnesium oxide is obtained. It is usually assumed that this material acts very much like a "perfect diffusor". Such a surface should look equally bright at all angles of observation. Its radiance would then have a constant value, independent of direction, or its intensity would follow Lambert's cosine law. This law yields

$$I_r(r) = \frac{\rho}{\pi} F_i \cos r \qquad (27)$$

where I_r is the intensity of the diffused light from the surface, r is the zenith angle of observation, ρ is the flux reflection coefficient of the surface, and F_i is the incident vertical light flux. In terms of radiance, the same law yields

$$L_r(r) = \frac{\rho}{\pi} E_i = \frac{\rho}{\pi} \int_{2\pi} L_i(i) \cos i \, d\omega \qquad (28)$$

Here E_i is the incident irradiance, and i is the angle of incidence of the radiance L_i.

If the surface is not a perfect diffuser, i.e. ρ is a function of i and r and the azimuth angle θ, then

$$L_r(i,r,\theta) = \frac{1}{\pi} \int_{2\pi} \rho(i,r,\theta) L_i(i,\theta) \cos i \, d\omega \qquad (29)$$

The mean value of ρ becomes

$$\bar{\rho} = \frac{\int_{2\pi} L_r \cos r \, d\omega}{\int_{2\pi} L_i \cos i \, d\omega} = \frac{1}{\pi} \frac{\int_{2\pi} \left(\int_{2\pi} \rho(i,r,\theta) L_i(i,\theta) \cos i \, d\omega \right) \cos r \, d\omega}{\int_{2\pi} L_i(i,\theta) \cos i \, d\omega} \qquad (30)$$

Such mean reflection coefficients of magnesium oxide have been measured in integrating spheres by BENFORD et al. (1948), MIDDLETON and SANDERS (1951) and TELLEX and WALDRON (1955).

In our work we need the value of $\rho(i,r,\theta)$ for $i=r=45^\circ$ and $\theta=0$. WORONKOFF and POKROWSKI (1923) have measured $\rho(i,r,0)$ in relative units. They find and increase in the forward scatterance for high values of i, and the best agreement with the cosine law for $i=0$. HARRISON's (1946) more detailed measurements of $\rho(r,i,0)$ reveal the same deviations for high i-values, but the best "cosine" agreement is obtained for $i = 45^\circ$. A few of his results have been used in the table below. The values of ρ are in relative units and normalized with $\rho(0,0) = 100$. CARR and ZIMM (1950) have measured

	$\rho(i,r)$					
r \ i	0°	15°	30°	45°	60°	75°
-75°	76	82	78	81		
-60°	84	86	87			
-45°	90	91				80
-30°	94				86	77
-15°				92	85	78
0°	(100)		95	92	85	76
15°		96	94	90	85	78
30°	94	92	92	91	88	84
45°	90	88	90	91	93	97
60°	82	83	86	92	105	128
75°	67	69	77	89	118	232

$\rho(45^\circ, r, 0)$ also in relative units. They point out that the absolute value of $\rho(r, 45^\circ, 0)$ may not be the same as the $\bar{\rho}$-value obtained from integrating spheres. Still, since they find no significant deviation from the cosine law in their measurements, they assume that the absolute values of $\rho(45^\circ, 45^\circ, 0)$ and $\bar{\rho}$ are almost equal. If this argument is not quite convincing, we may return to eq. 30. When L_i is constant, $\bar{\rho}$ may be re-written as

$$\bar{\rho} = \int_0^{90^\circ} \left(\int_0^{90^\circ} \bar{\rho}(i,r) \sin 2i \, di \right) \sin 2r \, dr \qquad (31)$$

where $\bar{\rho}(i,r)$ is the azimuthal mean of $\rho(i,r,\theta)$. Since sin 2i and sin 2r both have their maxima at 45°, it is likely that the integral will be dominated by the value of $\rho(45^\circ, 45^\circ)$, so that

$$\bar{\rho} \approx \bar{\rho}(45^\circ, 45^\circ) \qquad (32)$$

The present MgO coating was 2 mm thick, and from the measurements of TELLEX and WALDRON I have adapted the value $\rho = 0.96 \pm 0.02$ for all wavelengths.

4.1.2. The calibration formula

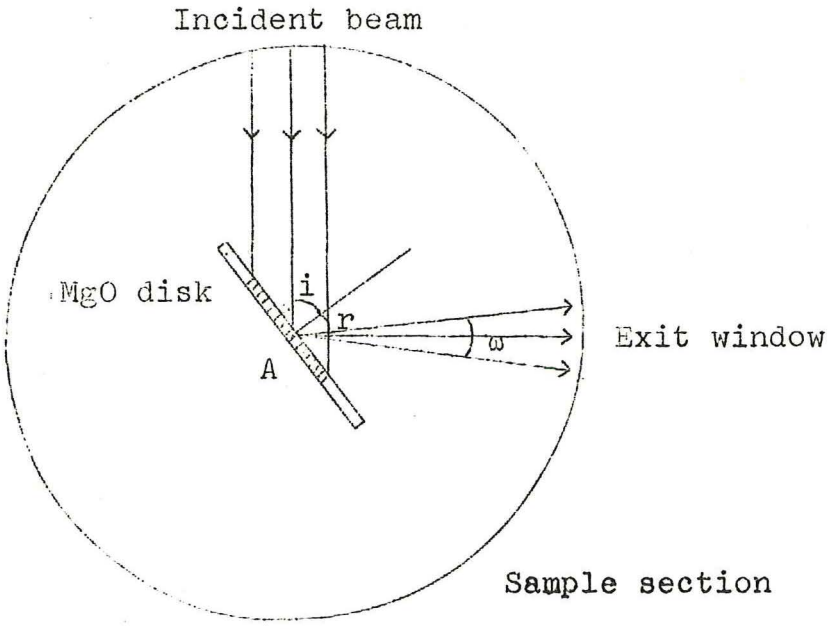

The MgO disk is placed vertically at the center of the empty sample section. The light beam's incidence angle at the MgO disk is i. It receives an irradiance

$$E = E_o \cos i \tag{33}$$

where E_o is the irradiance at an area normal to the beam. The radiance from the disk will have a value given by eq. 28,

$$L_r = \frac{\rho}{\pi} E = \frac{\rho}{\pi} E_o \cos i \tag{34}$$

The flux received by the photomultiplier is

$$F = L_r A \cos r \, \omega = \frac{\rho}{\pi} E_o \cos i \, A \cos r \, \omega \tag{35}$$

An important point is whether the area A which is observed by the photomultiplier is smaller or greater than the irradiated area. If it is smaller, then A cos r will remain constant when i is changed, and the instrument signal P will vary according to

$$P \sim F \sim \cos i \tag{36}$$

If A is greater than the irradiated area, then the effective area will be

$$A' = \frac{A_o}{\cos i} \tag{37}$$

where A_o is the cross section of the incident light beam, and the signal will vary according to

$$P \sim F \sim \cos r \tag{38}$$

A third possibility is that the border of the irradiated area is partly within and partly outside the photomultiplier's field of view. The effective

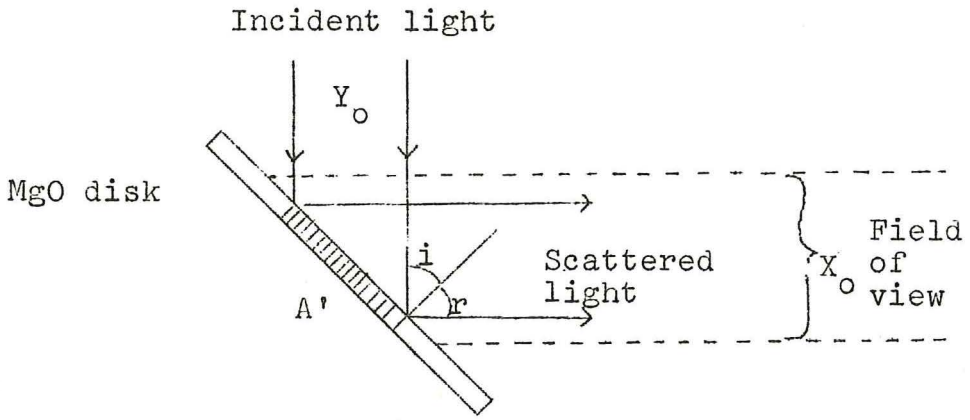

The disk seen from above

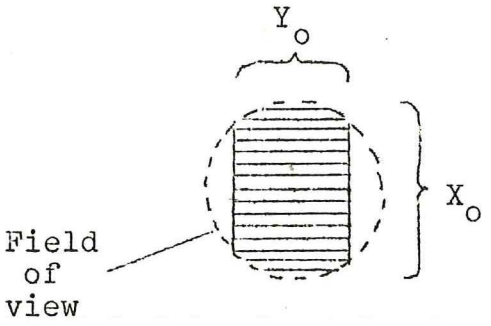

The disk seen from the photomultiplier

area will then be

$$A' = \left(\frac{X_o}{2}\right)^2 2(\text{Arcsin } u + u\sqrt{1-u^2}),$$

$$= \left(\frac{X_o}{2}\right)^2 \cdot f(u) \quad \text{for } u \leq 1,\ u = \frac{Y_o \cos r}{X_o \cos i}, \qquad (39)$$

where Y_o is the width of the incident beam and X_o is the diameter of the photomultiplier's field of view at the center of the sample cell.

The table of observations below illustrates that our case is closely described by eq. 36. The higher values of P/cos i for $i + r = 135^o$, are in accordance with the results presented in the table of the last chapter.

λ	i	r	P	P/cos i	P/cos r
546nm	45°	45°	25	35	35
	55°	35°	21	37	26
	65°	25°	15	36	17
	75°	15°	10	39	10
	67.5°	67.5°	20	52	52
	75°	60°	15	57	30
630nm	45°	45°	51	72	72
	70°	20°	25	74	27
	67.5°	67.5°	40	105	105

The small increase of P/cos i when i increases from 45°, is explained by eq. 39, and indicates that Y_o is slightly smaller than X_o. In fact, attempts to determine Y_o and X_o in air, give Y_o = (12±1) mm, X_o = (14.5±1) mm.

The signal measured with i = r = 45° is

$$P_{MgO} = F_a \tau_a S = \frac{\rho}{\pi} E_{oa} \cos^2 45^\circ A' \omega_a \tau_a S \qquad (40)$$

τ_a is the transmittance of the exit window/air interface. S is the sensitivity of the instrument.

When a sample bottle is placed at the center of the sample section and the space around the bottle is filled with clear water, the water inside the bottle will give a signal

$$P_W = F_W \tau_W S = \beta(90^\circ) E_{oW} v_W \omega_W \tau_W S \qquad (41)$$

by means of eqs. 1 and 2. The subscript w refers to values in water. Eqs. 40 and 41 give

$$\beta(90^\circ) = \frac{P_W}{P_{MgO}} \frac{\rho}{\pi} \frac{\tau_a}{\tau_W} \frac{E_{oa}}{E_{oW}} \frac{\omega_a}{\omega_W} \frac{A' \cos^2 45^\circ}{v_W} \qquad (42)$$

A' is related to the scattering volume in air v_a by

$$v_a = A' \cos 45^\circ X_{oa} = \pi \left(\frac{X_{oa}}{2}\right)^2 \cdot Y_{oa} \qquad (43)$$

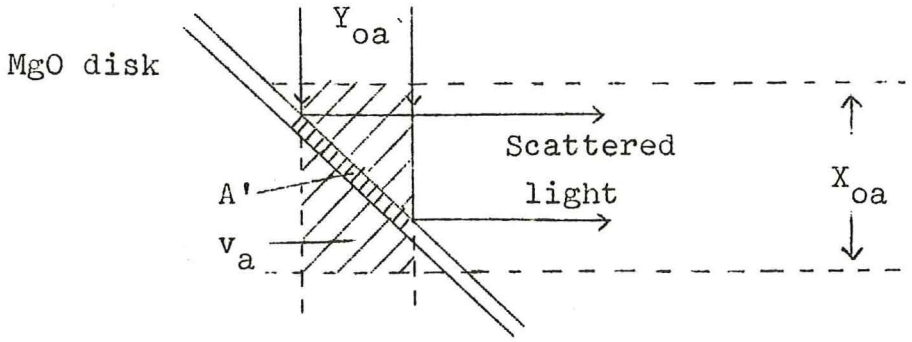

Y_{oa} is the width of the incident beam in air, and X_{oa} is the diameter of the cylindric observation field from the photomultiplier. Similarly the scattering volume in water will be

$$v_w = \pi \left(\frac{X_{ow}}{2}\right)^2 \cdot Y_{ow} \qquad (44)$$

If the lens and pinhole accept light in a solid angle ω_a in air, then the refraction between air and water will reduce this solid angle to

$$\omega_w = \omega_a / n_w^2 \qquad (45)$$

in water. n_w is the refractive index of water, relative to air. In the optical system described by COUMOU (1960), the product $n^2 \omega v$ is an instrumental constant, independent of the scattering medium. In our system $n^2 \omega$ is constant, but unfortunately v varies and has to be measured. By means of eqs. 39 and 43, eq. 42 becomes

$$\beta(90^\circ) = \frac{P_w}{P_{MgO}} \frac{\rho}{\pi} \frac{\tau_a}{\tau_w} \frac{E_{oa}}{E_{ow}} \frac{1}{n_w^2} \frac{f(u)}{\pi} \frac{X_{oa}^2 \cos 45^\circ}{X_{ow}^2 \, Y_{ow}} \qquad (46)$$

If the scattering angle in water is changed from 90° to 45°, the scattering volume will increase by a factor $1/\cos 45^{\circ}$.

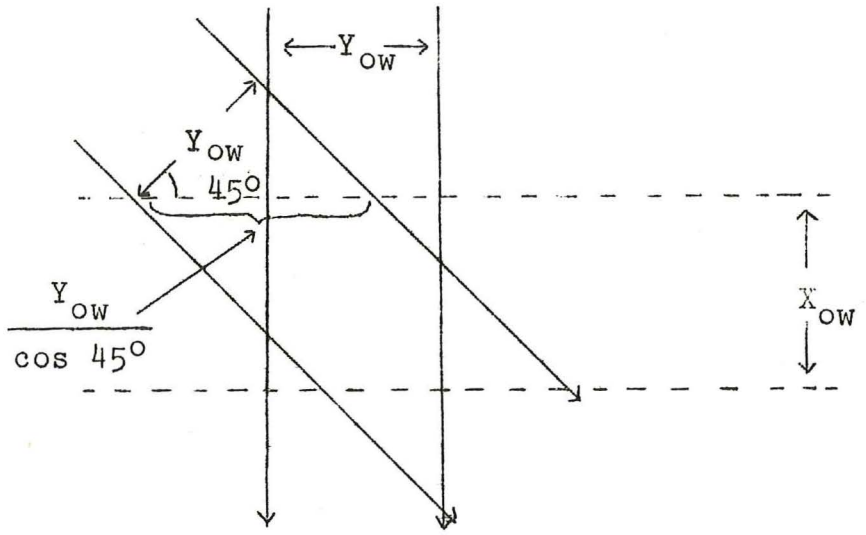

This effect is confirmed by measurements of the almost isotropic fluorescence from a solution of quinine sulfate. The mean value of different observations yields

$$\frac{P(45^{\circ})\cos 45^{\circ}}{P(90^{\circ})} = 0.98 \pm 0.03$$

The calibration formula for $\beta(45^{\circ})$ becomes

$$\beta(45^{\circ}) = \frac{P_w}{P_{MgO}} \frac{\rho}{\pi} \frac{\tau_a}{\tau_w} \frac{1}{n_w^2} \frac{E_{oa}}{E_{ow}} \frac{f(u)}{\pi} \frac{X^2_{oa}}{X^2_{ow}} \frac{\cos^2 45^{\circ}}{Y_{ow}} \qquad (47)$$

4.1.3. Estimates of the instrumental constants

In Chapter 4.1.1. we chose the value 0.96±0.02 for ρ. The value of $(\tau_a/\tau_w n^2_w)$ is from Fresnel's equation

$$\frac{(1 + \frac{n_g}{n_w})^2}{(1 + n_g)^2} \frac{1}{n_w} = 0.55 \pm 0.01$$

where n_g is the refractive index of glass.

E_{oa}/E_{ow} may be obtained from irradiance measurements or from the proportionality

$$\frac{E_{oa}}{E_{ow}} = \frac{A_{ow}\,\tau_a}{A_{oa}\,\tau_w} \tag{48}$$

where A_o as before is the cross-sectional area of the incident beam. τ is the transmittance of the interface between entrance window and sample cell. The first method gives $E_{oa}/E_{ow} = 0.94\pm0.07$, the other method 0.96 ± 0.05. The value 0.95 ± 0.05 is then chosen. The same measurements give $Y_{oa} \approx Y_{ow} = (12\pm1)$mm.

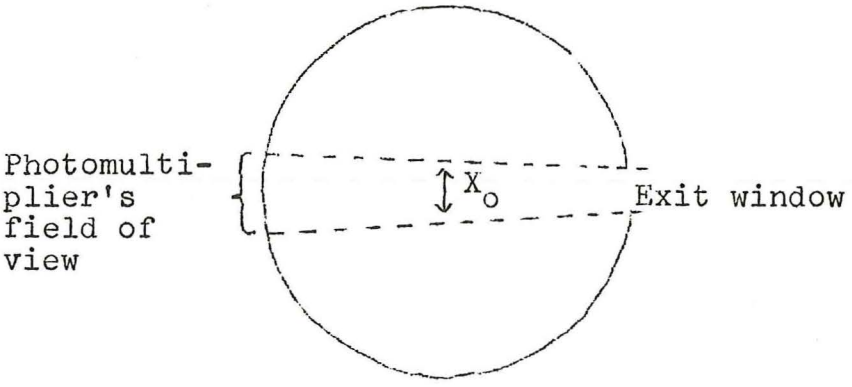

The photomultiplier's field of view was found by moving a white stick across the black wall of the sample section, while observing whether the photomultiplier reacted or not. X_o at the center of the cell could then be estimated. The values were $X_{oa} = (14.5\pm1)$mm and $X_{ow} = (11.5\pm1)$mm. We then get, by means of eq. 39,

$$\frac{f(u)X_{oa}^2\cos^2 45^\circ}{\pi\, X_{ow}^2\, Y_{ow}} = (0.60\pm0.15)\text{cm}^{-1}$$

Eq. 47 becomes

$$\beta(45^\circ) = \frac{P_w}{P_{MgO}}(10\pm3)\text{m}^{-1} \tag{49}$$

4.1.4. Calibration results

The measurements with the magnesium oxide disk were performed with $i=r=45^{\circ}$. For the filters B12 and O2 a neutral filter had to be added in order to reduce the signals. The signals from the standard were obtained with 45° scattering angle, and with water in the sample cell. The results, calculated from eq. 49, are presented below.

λ (nm)	366	406	546	578	630
$\beta_s(45^{\circ})(10^{-4}m^{-1})$	110±30	83±25	35±11	31±9	35±11

4.2. Method 2. The integrating MgO disk

4.2.1. The calibration formula

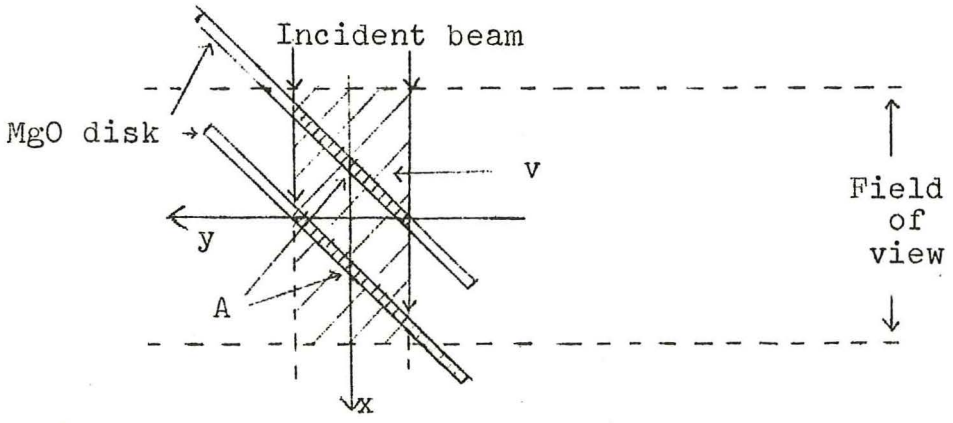

The signal produced by the MgO disk in an arbitrary position, with $i=r=45^{\circ}$, is

$$P_{MgO}(x,y) = F_a \tau_a S = \frac{\rho}{\pi} E_{oa}(x,y) A(x,y) \omega_a \cos^2 45^{\circ} \tau_a S \qquad (50)$$

At the center of the cell, $x=y=0$, this equation coincides with eq. 40. A, the part of the irradiated disk which is observed by the photomultiplier, may now vary in size according to its position. If the

disk is moved stepwise along the x axis and the corresponding signals are measured, one may integrate the signal and obtain

$$\int P_{MgO}(x,0)dx = \frac{\rho}{\pi}\,\omega_a \cos 45^\circ \tau_a S\,\overline{E_{oa}(x,0)}\int A(x,0)\cos 45^\circ dx, \tag{51}$$

where $\overline{E_{oa}(x,0)}$ is the mean value of the irradiance during the integration. But the last integral is v_a, the scattering volume in air. The equation becomes

$$\int P_{MgO}(x,0)dx = \frac{\rho}{\pi}\,\omega_a \cos 45^\circ\, \tau_a S\,\overline{E_{oa}(x,0)}\, v_a \tag{52}$$

It should be noted that

$$v_a = \int A(x,0)\cos 45^\circ dx = \int A(0,y)\cos 45^\circ dy \tag{53}$$

that is, the integral will obtain the same value whether we move the disk in the x or y direction. Consequently

$$\int P_{MgO}(x,0)dx = \int P_{MgO}(0,y)dy \tag{54}$$

Eqs. 41 and 51 give

$$\beta(90^\circ) = \frac{P_w}{\int P_{MgO}(x,0)dx}\,\frac{\rho}{\pi}\left(\frac{\overline{E_{oa}}\;\omega_a\; v_a}{E_{ow}\;\omega_w\; v_w}\right)\cos 45^\circ \tag{55}$$

It is seen that the great advantage of this method occurs if both measurements can be made in water, since the ratio in the parenthesis then will become 1. BLAKER et al. (1949) use a porcelain plate as a substandard in measurements of carbon disulfide. PRITCHARD and ELLIOT (1960) measure in air, and use a plastic screen with known optical properties. TYLER (1963) and FRY (1974) use plastic screens of unknown properties in water, but their procedures require facilities which the present instrument

does not have.

The calibration formula for $\beta(45^\circ)$ will by means of eqs. 43 and 44 become

$$\beta(45^\circ) = \frac{P_w}{\int P_{MgO}(x,0)dx} \frac{\rho}{\pi} \frac{\overline{E_{oa}}}{E_{ow}} \frac{\tau_a}{\tau_w n_w^2} \frac{X_{oa}^2 Y_{oa}}{X_{ow}^2 Y_{ow}} \cos^2 45^\circ \qquad (56)$$

4.2.2. Calibration results

The mean value of $P_{MgO}(x,0)$ is pictured in Fig. 6. The value of the integral may be written $P_{MgO}(0,0)\cdot(14.1\pm0.3)$mm, while the other quantities have the same values as in Chapter 4.1.3. The calibration formula now becomes

$$\beta(45^\circ) = \frac{P_w}{P_{MgO}(0,0)} (9\pm2)m^{-1} \qquad (57)$$

The integration was only performed at 630 nm, and P_w/P_{MgO} has the same value as was used in Chapter 4.1.4. The scattering function of the standard at 630 nm and 45° angle becomes with this method

$$\beta_s(45^\circ, 630 \text{ nm}) = (32\pm7)10^{-4}m^{-1}.$$

4.3. Method 3. The fluorescence of quinine sulfate

4.3.1. The calibration formula

The fluorescence of quinine in acid solutions is a commonly used reference, and will also be discussed in Chapter 5. The relation between the quantum efficiency Q and the spectral distribution of the fluorescent light has been expressed by eq. 12. It is convenient to introduce a normalized energy fluorescence distribution $f_{N\lambda}$ defined by

$$f_{N\lambda} = \frac{f_\lambda}{\int_{\lambda_x}^{\lambda_f} f_\lambda d\lambda} = \frac{f_\lambda}{a(\lambda_x)Q} \qquad (58)$$

The function $f_{N\lambda}$ for quinine sulfate and quinine bisulfate in solutions of H_2SO_4 is presented in Fig. 7. The values have been calculated from KORTÜM and FINCKH (1941), MELHUISH (1960), EASTMAN (1967) and PARKER (1968). The differences are significant, and are perhaps due to the source or prehistory of the quinine (MELHUISH, 1960) or to the acidity of the solutions (DAWSON and WINDSOR, 1968).

The value of Q was by MELHUISH (1961) calculated to 0.546. EASTMAN (1967) gives the value 0.58, and DAWSON and WINDSOR (1968) give the value 0.50±0.02 for a solvent of 0.1N H_2SO_4. The mean value (0.54±0.04) will be applied here.

The angular distribution of the fluorescence is given by a function similar to eq. 23

$$\phi(\theta) = \phi(90^\circ)(1 + \frac{1-\delta}{1+\delta} \cos^2\theta) \qquad (59)$$

By means of eq. 9

$$f = 4\pi\ \phi(90^\circ)(1 + \frac{1}{3}\frac{1-\delta}{1+\delta}) \qquad (60)$$

It is generally assumed that the fluorescence of quinine is isotropic. PERRIN (1929, p.260) shows that δ of quinine varies with the viscosity of the solvent, and that δ in water attains the value 1.00. My own measurements give $\delta = 0.98\pm0.02$. We may then apply for quinine

$$f = 4\pi\ \phi(90^\circ) = 4\pi\phi \qquad (61)$$

The signal from the fluorescent solution measured at 90° angle, will be

$$P_f = \int E(\lambda_x) e^{-c(\lambda_x)r} \phi_\lambda(\lambda_x,\lambda_f)\omega v \tau T_f(\lambda_f)S(\lambda_f)d\lambda_f \qquad (62)$$

where T_f is the transmittance of the applied exit filter, $c(\lambda_x)$ is the attenuation coefficient of the solution at λ_x, and r is the radius (2.5 cm) of the sample bottle. $c(\lambda_f)$ is neglected (see Fig. 8, $\lambda > 400$ nm). $c(\lambda_x) \simeq a(\lambda_x)$, since absorption dominates the attenuation at this wavelength. By substitutions from eqs. 58 and 60, eq. 62 becomes

$$P_f = E(\lambda_x) e^{-a(\lambda_x)r} \frac{a(\lambda_x)Q}{4\pi} \omega v \tau \int f_{N\lambda}(\lambda_f)T_f(\lambda_f)S(\lambda_f)d\lambda_f \qquad (63)$$

The signal from the plexi-glass standard, measured at 45° angle and at the excitation wavelength, is

$$P_s = E(\lambda_x)\beta_s(45^\circ,\lambda_x) \frac{\omega v}{\cos 45^\circ} \tau T_s(\lambda_x)S(\lambda_x) \qquad (64)$$

T_s is the exit filter applied to select the line at λ_x. v, as before, is the scattering volume at 90° observation angle.

From eqs. 63 and 64 the calibration formula is obtained

$$\beta_s(45^\circ,\lambda_x) = \frac{P_s}{P_f} \frac{a(\lambda_x)e^{-a(\lambda_x)r} Q \cos 45^\circ}{4\pi T_s(\lambda_x) S(\lambda_x)} \int f_{N\lambda}(\lambda_f)T_f(\lambda_f)S(\lambda_f)d\lambda_f \qquad (65)$$

4.3.2 Calibration results

The solution consisted of 1 mg of quinine sulfate in 0.01N H_2SO_4. The attenuation coefficient of the solution was measured at a spectrophotometer, and compared with distilled water. The difference was assumed to be the absorption coefficient of the quinine. The absorption curve is shown in Fig. 8. At 366 nm the

absorption coefficient is 1.93 m^{-1}, consistent with the value 2.01 m^{-1} which may be computed from the data given by PARKER (1968, table 47).

The solution was irradiated by light at 366 nm, by means of the entrance UV filter. The fluorescence was measured at 90° angle and with three different filters at the exit: the usual V9 filter with maximum transmittance at 525 nm, a G5 filter which cuts off light below 440 nm, and a Wratten 2B filter which cuts off light below 400 nm. The $f_{N\lambda}$ functions from KORTÜM & FINCKH and MELHUISH, which constitute the extreme values in Fig. 7, were chosen for the calculations.

The scattered light from the plexi-glass standard was measured at 45° angle, with the UV filter at the entrance and the B12 filter at the exit. The transmittance of the employed filters were measured at a spectrophotometer. The ratio between $S(\lambda_f)$ and $S(\lambda_x)$ was obtained from the relative sensitivity curve in Fig. 3.

The table below gives the results calculated from eq. 65. The mean value is $(137\pm25)\cdot10^{-4}m^{-1}$.

	$\beta_s(45^{\circ},366\text{ nm})$ $(10^{-4}m^{-1})$	
Filter	$f_{N\lambda}$ due to KORTÜM & FINCKH	$f_{N\lambda}$ due to MELHUISH
V9	98±10	153±15
G5	132±13	140±14
2B	160±16	139±14

4.4. Method 4. Rayleigh scatterance at two angles with tin reflectance.

4.4.1. The Rayleigh scatterance of water.

The molecular or Rayleigh scattering function is given by eq. 23. The constants in the equation are the depolarization ratio δ of water, and $\beta_w(90^{\circ},\lambda)$ of water (also termed the Rayleigh ratio). MOREL in 1974

reviewed some of the earlier obtained values of δ. Later values are by PIKE et al. (1975), who have found $\delta = 0.076$ at 633 nm, and by FARINATO and ROWELL (1976) who find $\delta = 0.051$ at 515 nm. However, I have chosen the same value as MOREL, $\delta = 0.09$ for all wavelengths.

We may write

$$\beta_w(90^o, \lambda) = \beta_w(90^o, \lambda_o)\, R(\lambda, \lambda_o) \qquad (66)$$

where λ_o is a fixed wavelength, e.g. 366 nm. According to MOREL (1974), $\beta_w(90^o, 366\ \text{nm})$ is $5.32 \cdot 10^{-4} m^{-1}$, and the function $R(\lambda)$ may also be calculated from MOREL's data (Fig. 9). Eq. 23 then gives

$$\beta_w(\theta,\lambda) = R(\lambda)(1 + 0.835 \cos^2\theta) \cdot 5.32 \cdot 10^{-4} m^{-1} \qquad (67)$$

4.4.2. The reflectance of tin in water

The applied formula of metallic reflectance is (KÖNIG, 1928)

$$\rho = \frac{A - B \cos i + \cos^2 i}{A + B \cos i + \cos^2 i} \cdot \frac{A + \sin^2 i \tan^2 i}{A + B \sin i \tan i + \sin^2 i \tan^2 i} \qquad (68)$$

where

$$A = \sqrt{(n^2 - k^2 - \sin^2 i)^2 + 4 n^2 k^2} \qquad (69)$$

$$B = \sqrt{2A + 2(n^2 - k^2 - \sin^2 i)} \qquad (70)$$

Here i is the angle of incidence in water, n is the refractive index of tin relative to water, and k is a dimensionless coefficient of absorption. The refractive index and absorption coefficient of tin and the refractive index of water, were derived from LANDOLT - BÖRNSTEIN (1962, 2/8, p. 1-14 and p. 5-565). The reflectances for observation angles of 45^o ($i = 67.5^o$)

and 90° ($i = 45^{\circ}$) are presented in Fig. 9. The values will be used in this and a later calibration method.

4.4.3 The calibration formula

The signal of a sample which scatters light at 90° angle, will be

$$\begin{aligned} P(90^{\circ}) &= FS = E\,\beta(90^{\circ})\omega\, v\, \tau\, T\, S \\ &= E\{\beta_w(90^{\circ}) + \beta_p(90^{\circ})\}\omega\, v\, \tau\, T\, S \end{aligned} \tag{71}$$

where β_w is the molecular or Rayleigh part of the scattering function, due to the pure water, and β_p is the part due to particles. Similarly we may write

$$P(45^{\circ}) = E\{\beta_w(45^{\circ}) + \beta_p(45^{\circ})\}\frac{\omega\, v\, \tau}{\cos 45^{\circ}}\, T\, S \tag{72}$$

We shall make the assumption that α_w and α_p, defined by

$$\alpha_w = \frac{\beta_w(45^{\circ})}{\beta_w(90^{\circ})\cos 45^{\circ}} \tag{73}$$

$$\alpha_p = \frac{\beta_p(45^{\circ})}{\beta_p(90^{\circ})\cos 45^{\circ}} \tag{74}$$

are constants independent of wavelength. Substitutions from eqs. 66, 71, 73 and 74 in eq. 72 give

$$P(45^{\circ},\lambda) = E(\alpha_w-\alpha_p)\beta_w(90^{\circ},\lambda_o)R(\lambda)\omega\, v\, \tau\, T\, S + \alpha_p P(90^{\circ},\lambda) \tag{75}$$

which also may be written

$$\frac{P(45^{\circ},\lambda)}{ERTS} = (\alpha_w-\alpha_p)\beta_w(90^{\circ},\lambda_o)\omega\, v\, \tau + \alpha_p\frac{P(90^{\circ},\lambda)}{ERTS} \tag{76}$$

This equation is of the form

$$y(\lambda) = A + B\, x(\lambda) \tag{77}$$

where A and B are constants independent of wavelength.

The unknown part in y and x is the product ETS. Its relative variation with λ is that of the signals from a neutral scatterer. To determine this variation, I have used the metallic reflectance of tinned electronic copperwire. The wire will give steady signals, and the amount of light may be controlled by the amount of wire which is irradiated. The signals due to the tinned copper wire will be

$$P_t(\lambda) \sim \rho(\lambda)E(\lambda)T(\lambda)S(\lambda) \tag{78}$$

where ρ is the reflectance given in Chapter 4.4.2. Measurements at different wavelengths give

$$\frac{P_t(\lambda)}{P_t(\lambda_o)} = \frac{\rho(\lambda)E(\lambda)T(\lambda)S(\lambda)}{\rho(\lambda_o)E(\lambda_o)T(\lambda_o)S(\lambda_o)} \tag{79}$$

or

$$E(\lambda)T(\lambda)S(\lambda) = E(\lambda_o)T(\lambda_o)S(\lambda_o)\,\frac{\rho(\lambda_o)}{\rho(\lambda)}\,\frac{P_t(\lambda)}{P_t(\lambda_o)} = k_o F(\lambda) \tag{80}$$

where

$$k_o = E(\lambda_o)T(\lambda_o)S(\lambda_o) \tag{81}$$

and

$$F(\lambda) = \frac{\rho(\lambda_o)}{\rho(\lambda)}\,\frac{P_t(\lambda)}{P_t\lambda_o} \tag{82}$$

Eq. 76 becomes

$$\frac{P(45^o,\lambda)}{F(\lambda)R(\lambda)} = k_o(\alpha_w-\alpha_p)\beta_w(90^o,\lambda_o)\omega\, v\, \tau + \alpha_p\,\frac{P(90^o,\lambda)}{F(\lambda)R(\lambda)} \tag{83}$$

Repeated measurements of $P_t(\lambda)/P_t(\lambda_o)$, corrected for the contributions from the water, and multiplied with $\rho(\lambda)/\rho(\lambda_o)$, were used to determine the mean values of $F(\lambda)$. Eqs. 67 and 73 give $\alpha_w = 2.00$. We now have

the sufficient information to calculate the variables in eq. 77.

$$y(\lambda) = P(45^{\circ},\lambda)\ \frac{1}{F(\lambda)R(\lambda)} \tag{84}$$

$$x(\lambda) = P(90^{\circ},\lambda)\ \frac{1}{F(\lambda)R(\lambda)} \tag{85}$$

$$A = k_o(2.00-\alpha_p)\omega\ v\ \tau \cdot\ 5.32\cdot10^{-4}m^{-1} \tag{86}$$

$$B = \alpha_p \tag{87}$$

The signal from the plexi-glass standard at λ and 45° angle, is

$$P_s(45^{\circ},\lambda) = E(\lambda)\beta_s(45^{\circ},\lambda)\ \frac{\omega v(90^{\circ})}{\cos 45^{\circ}}\tau\ T(\lambda)S(\lambda) \tag{88}$$

When this equation is solved for β_s, and eqs. 74, 86 and 87 are utilized, we obtain the calibration formula

$$\beta_s(45^{\circ},\lambda) = \frac{P_s(45^{\circ},\lambda)}{F(\lambda)}\ \cos 45^{\circ}\ \frac{(2.00-B)}{A}\ 5.32\cdot10^{-4}m^{-1} \tag{89}$$

Eqs. 72 and 88 give

$$\beta_p(45^{\circ},\lambda) = \beta_s\ \frac{P(45^{\circ},\lambda)}{P_s(45^{\circ},\lambda)} - \beta_w(45^{\circ},\lambda) \tag{90}$$

The advantage of this method compared with the next one, is that A and B will remain constant even if the particle content decreases.

4.4.4. The calibration results

Double distilled water (which may contain a lot of particles), was used for the calibration. The signals were measured for 5 wavelengths and for the two scattering angles. The measurements were repeated.

The signals were slowly decreasing, due to sinking of the particles. The calculated values of y (eq. 84) and x (eq. 85) are shown in Fig. 10. The method of the least squares gives A = -3.45, B = 37.9. Eqs. 89 and 90 give

λ(nm)	366	406	436	546	578	630
$\beta_s(45^\circ)(10^{-4}m^{-1})$	117±23	92±18	76±16	47±9	38±8	41±1
$\beta_p(45^\circ(10^{-4}m^{-1})$	52±4	50±4	55±7	50±4	47±5	50±4

It is interesting that within the accuracy of the measurement, no dispersion in the particle scatterance is detected. A surprising result, however, is that α_p is 37.9, which makes $\beta_p(45^\circ)/\beta_p(90^\circ)$ = 26.8. For natural water the ratio is usually about 7 (JERLOV, 1976, p. 37). The present particles are probably not "natural", but originate from the silica destillation apparatus. When viewed in a microscope, they seem to have the form of flakes, with lengths of maximum axes between 10 and 40 µm. If they are not distributed at random while sinking, but have their main axes in the horizontal plane (like leaves falling from a tree), then perhaps forward refraction of light through the particles may lead to the high ratio.

4.5. Method 5. Rayleigh scatterance at two angles with neutral particle scatterance

4.5.1. The calibration formula

In the preceding section the only requirement on the particle scattering was that its angular distribution, expressed by α_p, should be independent of wavelength. If we also assume that the scatterance is non-dispersive

(which is justified by the results in Chapter 4.4.4), the procedure becomes simpler. Substitution of E ωv TS from eq. 71 into eq. 72 gives, by means of eqs. 73 and 74

$$(1-\alpha_w \frac{P(90^o,\lambda)}{P(45^o,\lambda)})R(\lambda) = -\frac{\beta_p(90^o)}{\beta_w(90^o,\lambda_o)} + \alpha_p \frac{\beta_p(90^o)}{\beta_w(90^o,\lambda_o)} \frac{P(90^o,\lambda)}{P(45^o,\lambda)} \quad (91)$$

This equation is similar to eq. 77, with

$$y(\lambda) = (1-\alpha_w \frac{P(90^o,\lambda)}{P(45^o,\lambda)})R(\lambda) \quad (92)$$

$$x(\lambda) = \frac{P(90^o,\lambda)}{P(45^o,\lambda)} \quad (93)$$

$$A = -\frac{\beta_p(90^o)}{\beta_w(90^o,\lambda_o)} \quad (94)$$

$$B = \alpha_p \frac{\beta_p(90^o)}{\beta_w(90^o,\lambda_o)} = \frac{\beta_p(45^o)}{\beta_w(90^o,\lambda_o)\cos 45^o} \quad (95)$$

The signal from the standard, P_s, is given by eq. 88. With eqs. 71 and 94 we get

$$\beta_s(45^o,\lambda) = \beta_w(90^o,\lambda_o)[R(\lambda)-A]\cos 45^o \frac{P_s(45^o,\lambda)}{P(90^o,\lambda)} \quad (96)$$

The disadvantage with this method is that A and B vary with the particle content. Since the content gradually decreases during the series, the points obtained are less likely to lie on a straight line.

4.5.2. The calibration results

The values of y (eq. 92) are plotted as a function of x (eq. 93) in Fig. 11. Linear regression analyses give A = -0.330 and B = 12.9. From eqs. 95 and 96 we get

λ (nm)	366	406	436	546	578	630
$\beta_s(45^o,\lambda)(10^{-4}m^{-1})$	115±5	84±5	75±13	43±3	40±3	42±11
$\beta_p(45^o)(10^{-4}m^{-1})$	49±11					

The results coincide well with the values of the last chapter.

4.6. Method 6. Rayleigh scatterance at one angle with tin reflectance

4.6.1. The calibration formula

The signal due to scattering at an angle θ, is

$$P(\theta,\lambda) = E(\lambda)\left(\beta_p(\theta,\lambda)+\beta_w(\theta,\lambda)\right)\omega\ v\ \tau\ T(\lambda)S(\lambda) \qquad (97)$$

which by means of eq. 80 may be written

$$\frac{P(\theta,\lambda)}{F(\lambda)} = k_o\ \omega\ v\ \tau\ \beta_p(\theta,\lambda) + k_o\ \omega\ v\ \tau\ \beta_w(\theta,\lambda) \qquad (98)$$

Provided β_p is independent of the wavelength, this equation is of the form

$$y(\lambda) = A + Bx(\lambda) \qquad (99)$$

However, if

$$\beta_p(\theta) >> \beta_w(\theta,\lambda) \qquad (100)$$

then

$$y(\lambda) \approx A \tag{101}$$

and it is not possible to determine B with sufficient accuracy. It is necessary for this method that θ has a value where the scattering functions of particles and water are of the same order of magnitude. Our measurements are therefore restricted to $\theta = 90^{\circ}$.

If the amount of irradiated particles decreases during the series of measurements, A will decrease while Bx remains constant. This will lead to a scattering of the points in the x-y diagram.

The points are given by

$$y(\lambda) = \frac{P(90^{\circ},\lambda)}{F(\lambda)} \tag{102}$$

$$x(\lambda) = \beta_w(90^{\circ},\lambda) \tag{103}$$

where $F(\lambda)$ is the earlier obtained function from measurements with tinned wire (eq. 82). Linear regression analyses give the values of

$$A = k_o\ \omega\ v\ \tau\ \beta_p(90^{\circ}) \tag{104}$$

and

$$B = k_o\ \omega\ v\ \tau \tag{105}$$

The signal from the standard is given by eq. 88, and the equation may be transformed to

$$\beta_s(45^{\circ},\lambda) = \frac{P_s(45^{\circ},\lambda)\cos 45^{\circ}}{F(\lambda)k_o\ \omega\ v\ \tau} = \frac{P_s(45^{\circ},\lambda)\cos 45^{\circ}}{F(\lambda)B} \tag{106}$$

The particle scattering function at 90° is

$$\beta_p(90^{\circ}) = \frac{A}{B} \tag{107}$$

4.6.2. Calibration results

The calculated y and x values are presented in Fig. 12. It is obtained that A = 0.0328 and B = 180 m, and that $\beta_p(90^\circ) = (1.8\pm0.2)\cdot10^{-4}m^{-1}$. The last result agrees well with the corresponding values which may be found from Method 4 and 5, $(1.9\pm0.2)\cdot10^{-4}m^{-1}$ and $(1.8\pm0.3)\cdot10^{-4}m^{-1}$ respectively.

The values of the standard scatterance become

λ (nm)	366	406	436	546	578	630
$\beta_s(10^{-4}m^{-1})$	115±5	90±4	84±4	46±3	37±2	40±3

4.7. Comparison of the methods

The different methods agree fairly well, as seen in the table below. Some of the similarity between the

	$\beta_s(45^\circ)$ $(10^{-4}m^{-1})$					
λ (nm)	366	406	436	546	578	630
Method 1	110±30	83±25		35±11	31±9	35±11
Method 2						32±7
Method 3	137±25					
Method 4	117±10	92±8	76±7	47±4	38±3	41±4
Method 5	115±7	84±7	75±13	43±5	40±5	42±10
Method 6	115±5	90±4	84±4	46±3	37±2	40±3
Mean of all methods	119±8	87±7	78±5	43±3	37±3	38±3
Fluorescence corrected values				40±3	36±2	29±3

values of Method 4, 5 and 6, may be due to the fact that they are calculated from the same data set.

By method 1 and 2 it is not necessary to know the spectral transmittance of the filters or the spectral sensitivity of the instrument. One must, however, determine the ratio between the scattering volumes, solid angles to the photomultiplier, and irradiances in air and water, and this is not easy to do with precision. Another disadvantage is that the use of the magnesium oxide disk leads to very high signals. These can either be reduced with neutral filters, but the accurate transmittance of these may be difficult to determine, or the high voltage over the photomultiplier can be lowered, but this may also introduce some inexactness. However, Method 2 should be very good when it can be executed entirely in water.

Method 3 has the advantage that it is not necessary to determine any geometrical quantities, but the relative spectral sensitivity of the instrument and the spectral transmittance of the filters must be known. It calibrates the standard only at the excitation wavelength, but if it is combined with a relative spectral calibration, like the tin calibration, it may give absolute values at all wavelengths. There are some doubts, however, whether the properties of quinine sulfate are constant enough for very exact calibrations.

By Method 4, 5 and 6 none of the properties of the instrument need to be known. Method 4 is probably the best, since its only assumption about the particle scattering is that the relative angular distribution shall be independent of wavelength.

Fig. 13 illustrates how the mean values of the table lie on a straight line in a double-logarithmic diagram, when the values at 546, 578 and 630 nm have been corrected for fluorescence, as discussed in Chapter 2.3. The relation between the scatterance and the wavelength, expressed by the straight line, is

$$\beta_s(45^\circ,\lambda) = \left(\frac{2326\ \text{nm}}{\lambda}\right)^{2.58} \cdot 10^{-4}\,\text{m}^{-1} \qquad (108)$$

5. FLUORESCENCE CALIBRATION

5.1. The fluorescence function in absolute units

Usually fluorescence is measured in 90° angle, with the UV filter at the entrance to select the line at 366 nm, and with the V9 filter with gravity center at 525 nm at the exit.

With this set-up, the plexiglass standard will give a signal

$$P_f = E(\lambda_x)\omega\, v\, \tau \int_{V9} \phi_\lambda(90^{\circ},\lambda_x,\lambda_f)T_{V9}(\lambda_f)S(\lambda_f)d\lambda_f$$

$$= E(\lambda_x)\omega\, v\, \tau\, \overline{\phi_\lambda(90^{\circ},\lambda_x,\lambda_f)} \int_{V9} T_{V9}(\lambda_f)S(\lambda_f)d\lambda_f \qquad (109)$$

When the 45° scatterance of the standard at λ_x = 366 nm is measured with the filter B12 at the exit, then

$$P_s = E(\lambda_x)\beta_s(45^{\circ},\lambda_x)\omega\, v\, \tau\, T_{B12}(\lambda_x)S(\lambda_x) \qquad (110)$$

From these equations ϕ_λ becomes

$$\phi_\lambda(90^{\circ},366\text{ nm},525\text{ nm}) = \overline{\phi_\lambda} = \frac{P_f}{P_s}\,\frac{\beta_s(45^{\circ},\lambda_x)T_{B12}(\lambda_x)S(\lambda_x)}{\cos 45^{\circ}\int_{V9} T_{V9}S d\lambda} \qquad (111)$$

The measurements give that the fluorescence function of the standard is

$$\phi_\lambda(90^{\circ},366\text{ nm},525\text{ nm}) = (176\pm8)\cdot10^{-8}\,m^{-1}nm^{-1} \qquad (112)$$

The choice of the V9 filter may be discussed. Its gravity center (525 nm) lies perhaps at a too long wavelength compared with the fluorescence peak of natural waters, which seems to be between 420 and 510 nm (KULLENBERG and NYGARD, 1971, BROWN, 1974, DUURSMA, 1974).

5.2. The fluorescence function relative to the Raman scatterance

BROWN (1974) discusses the use of the Raman scatterance of pure water as a reference standard. He suggests that it is used only as a convenient alternative to control the instrumental sensitivity. However, since it sometimes may be easier to compare a fluorescence with a Raman scatterance rather than to calibrate the fluorometer in absolute units, the method shall be discussed more closely here.

If the Raman scatterance of water is measured with a monochromator, the peak value of the spectral curve depends on the slit width. Consequently one should use the integrated value of the Raman scatterance, rather than the apparent peak value itself.

The signal at our instrument of the Raman scatterance at 418 nm, when the double distilled water is irradiated with light at 366 nm, and with the BR filter at the exit, is

$$P = E(\lambda_x)\omega\ v\ \tau \int_{BR} \beta_{R\lambda}(\lambda_x,\lambda_R)T_{BR}(\lambda_R)S(\lambda_R)d\lambda_R \qquad (113)$$

$\beta_{R\lambda}(\lambda_R)$ is the apparent spectral distribution of the Raman scatterance around 418 nm.

The signal due to scatterance from the standard with the filter B12 at the exit, is

$$P_s = E(\lambda_x)\beta_s(\lambda_x)\omega\ v\ \tau\ T_{B12}(\lambda_x)S(\lambda_x) \qquad (114)$$

A relative distribution $\beta'_{R\lambda}$ of the Raman scattering function is given by MOREL (according to DUURSMA, 1974, p.247) (Fig. 14). The ratio between the absolute and relative distributions may be termed k, so that

$$\beta_{R\lambda} = k\ \beta'_{R\lambda} \qquad (115)$$

From eqs. 113-115 we obtain

$$k = \frac{P}{P_s}\ \frac{\beta_s(\lambda_x)T_{B12}(\lambda_x)S(\lambda_x)}{\int \beta'_{R\lambda}T_{BR}S\ d\lambda} \qquad (116)$$

$\beta'_{R\lambda}$ is corrected for the background fluorescence of the double distilled water, as indicated in Fig.14. A question here is whether this fluorescence may be regarded as a constant or not. PRINGSHEIM and VOGEL (1946, p.68) say that distilled water emits an easily visible fluorescence when excited with ultraviolet light, that repeated distillations make the fluorescence weaker, but that it seems impossible to make the fluorescence disappear completely. However, I have assumed that the background fluorescence in my measurements is the same as it seems to be in MOREL's curve. This fluorescence contributes less than 15% to the signal.

When k is determined from eq. 116, the integrated Raman scatterance is found by

$$\beta_R = \int \beta_{R\lambda} d\lambda = k \int \beta'_{R\lambda} d\lambda \qquad (117)$$

In this way it seems that the Raman scatterance of pure water, due to irradiance at 366 nm, is

$$\beta_R(90^\circ, 366 \text{ nm}, 418 \text{ nm}) = (97 \pm 10) \cdot 10^{-6} \text{m}^{-1} \qquad (118)$$

The fluorescence function of the plexi-glass standard relative to the spectrally integrated function is by means of eqs. 112 and 118

$$\frac{\phi_\lambda(90^\circ, 366 \text{ nm}, 525 \text{ nm})}{\beta_R(90^\circ, 366 \text{ nm}, 418 \text{ nm})} = (18 \pm 2) \cdot 10^{-3} \text{nm}^{-1} \qquad (119)$$

The depolarization ratio of the Raman scatterance changes through the spectrum, as shown by WESTON (1962), MURPHY and BERNSTEIN (1972), and CUNNINGHAM and LYONS (1973). Fig. 15 shows $\beta'_{R\lambda}(90^\circ, \lambda)$ and $\delta(\lambda)$, calculated from the values of CUNNINGHAM and LYONS. Further calculations on these functions give that, by means of eq. 24,

$$b_R = \int\int \beta_{R\lambda} d\lambda \, d\omega = 4\pi \, \beta_R(90^\circ) 1.20 \qquad (120)$$

With the value in eq. 118, b_R becomes

$$b_R(366\ \text{nm}, 418\ \text{nm}) = (15\pm2)\cdot10^{-4}\text{m}^{-1} \qquad (121)$$

This value is about 17% of the Rayleigh scattering coefficient of water $b_w(366\ \text{nm}) = 87\cdot10^{-4}\text{m}^{-1}$, but it is much smaller compared with the absorption coefficient $a_w(366\ \text{nm}) \geqq 0.5\ \text{m}^{-1}$ (MOREL, 1974).

It may be noted that the spectral mean value of δ (weighted by $\beta_{R\lambda}$), is 0.28, and that resembling values have been measured by CABANNES and RIOLS (1934) and by PRICE et al. (1962).

The only attempt I have found to estimate the absolute value of the Raman scatterance of water, was by EISENBRANDT (1954). He compared the intensity of the Raman scatterance with the intensity of a certain concentration of a fluorescent substance, excited by the same line at 366 nm. By measuring the absorption coefficient of the fluorescent matter (sodium hydroxypyrene-trisulfonate) at 366 nm, and by assuming that the fluorescent matter had a 100% energy efficiency, and that the angular intensity distributions of fluorescence and Raman scattering were equal, he obtained

$$b_R \approx 1\cdot10^{-3}\text{m}^{-1}\ln 10 \approx 2\cdot10^{-3}\text{m}^{-1} \qquad (122)$$

From his data a more careful calculation may give the value $(21\pm2)\cdot10^{-4}\text{m}^{-1}$. However, a fluorescence energy efficiency of 100% is not possible. The fluorescence spectrum had its peak value at 510 nm, and even with a 100% quantum efficiency, b_R must be reduced by a factor $^{366}/_{510}$. EISENBRANDT observed the intensities at 90° angle. If the intensity distribution of the fluorescence is isotropic (eq. 61), and the Raman scatterance follows eq. 120, b_R should also be increased by a factor 1.20. EISENBRANDT's value is then changed to

$$b_R = (21\pm2)\cdot10^{-4}m^{-1}\ \frac{366}{510}\ 1.20 = (18\pm2)10^{-4}m^{-1} \qquad (123)$$

This corresponds rather well with the present value of $(15\pm2)\cdot10^{-4}m^{-1}$. The values would have been equal if the quantum efficiency of EISENBRANDT's fluorescent matter had been 15/18, or (83±14)%, and this is perhaps a more reasonable efficiency. The similarity between eqs. 121 and 123 supports the present measurements.

5.3. The fluorescence function relative to the fluorescence of quinine

A classic standard in spectrofluorometry is quinine in acid solutions. Quinine is often applied in the form of quinine bisulfate

$(C_{20}H_{24}N_2O_2)(H_2SO_4)(H_2O)_7$ (molar weight 548.60),

quinine sulfate

$(C_{20}H_{24}N_2O_2)_2\ (H_2SO_4)(H_2O)_2$ (molar weight 782.97),

or quinidine sulfate

$(C_{20}H_{24}N_2O_2)_2\ (H_2SO_4)(H_2O)_2$ (molar weight 782.93).

KALLE (1951) was the first to introduce it for seawater measurements. He gave a solution of 0.1 mg quinine bisulfate in 1 litre of 0.01 N H_2SO_4, the value 73 m.Fl. (KALLE, 1963) (m.Fl. is an abbreviation of microfluorescence value).

A solution of 1 mg quinine sulfate in 0.01 N H_2SO_4 gives a signal at our instrument which relative to the standard is 54±1. From the chemical formulas it may be deduced that 0.71 mg quinine sulfate will produce the same fluorescence as 1 mg quinine bisulfate. A signal

of 39 relative to the standard should then correspond to 730 m.Fl. However, KALLE applies visual observations of the total fluorescence spectrum, while the green filter V9 is used here, and this makes a comparison with his results difficult.

It may be doubted from the discussion in Chapter 4.3.1 whether the fluorescence of quinine is a suitable standard. But its good properties should not be forgotten: Its absorption and fluorescence spectra do not overlap, and the spectra are fairly smooth.

5.4. The angular distribution of fluorescence in natural waters

The distribution follows eq. 59, and from measurements at 45° and 90°, δ becomes

$$\delta = \frac{3 - 2\,\frac{\phi(45^\circ)}{\phi(90^\circ)}}{2\,\frac{\phi(45^\circ)}{\phi(90^\circ)} - 1} \qquad (124)$$

δ may also be measured directly, by means of a polaroid filter. The table below gives the depolarization factor for tap water with a high fluorescence, and winter Oslofjord water with a lower fluorescence.

	$\phi_\lambda(90^\circ, 525\ \text{nm})$ $10^{-7}\,\text{m}^{-1}\,\text{nm}^{-1}$	δ(polaroid filter) %	δ(Eq.124) %	Applied δ %
Tap water	45±2	94±2	97±3	95±3
Fjord water	17±1	91±4	91±8	91±4

For tap water we obtain by means of eq. 60

$$f_\lambda = 4\pi \, \phi_\lambda(90^\circ)1.009 \tag{125}$$

and for fjord water

$$f_\lambda = 4\pi \, \phi_\lambda(90^\circ)1.016 \tag{126}$$

It then seems that the emission of fluorescence in natural waters practically may be regarded as isotropic.

ACKNOWLEDGEMENTS

I want to thank KJELL NYGÅRD at the University of Copenhagen for his construction of the instrument. I am also due thanks to a lot of people, too numerous to name, from the Institutes of Chemistry, Marine Biology, Pharmacy and Physics at the University of Oslo, and from the Institute of General Physics at the Norwegian Institute of Technology (NTH), all of whom have given assistance and advice during this work.

REFERENCES

BENFORD, F., LLOYD, G.P. and SCHWARZ, S., 1948. Coefficients of reflection of magnesium oxide and magnesium carbonate. J.O.S.A., 38: 445-447.

BLAKER, R.H., BADGER, R.M. and GILMAN, T.S., 1949. The investigation of the properties of nitrocellulose molecules in solution by light-scattering methods. I. J. Phys. & Colloid Chem., 53: 794-803.

BROWN, M., 1974. Laboratory measurements of fluorescence spectra of Baltic waters. Rep. Inst. Phys. Oceanogr., Univ. Copenhagen. 29. 31 pp.

CABANNES, J., 1920. Relation entre le degré de polarisation et l'intensité de la lumière diffusée par des molécules anisotropes. Nouvelle détermination de la constante d'Avagadro. J. Phys. 6: 129-142.

CABANNES, J., and RIOLS, J. de, 1934. Effet Raman. Sur le spectre Raman de l'eau. Comt. Rend., 198: 30-32.

CARR, C.I., Jr. and ZIMM, B.H., 1950. Absolute intensity of light scattering from pure liquids and solutions. J.Chem.Phys., 18: 1616-1626.

COHEN, G. and EISENBERG, H., 1965. Light scattering of water, deuterium oxide, and other pure liquids. J.Chem.Phys., 43: 3881-3887.

COUMOU, D.J., 1960: Apparatus for the measurement of light scattering in liquids. Measurement of the Rayleigh factor of benzene and of some other pure liquids. J.Colloid Sci., 15: 408-417.

CUNNINGHAM, K. and LYONS, P.A., 1973. Depolarization ratio studies on liquid water. J.Chem.Phys., 59: 2132-2139.

DAWSON, W.R. and WINDSOR, M.W., 1968. Fluorescence yield of aromatic compounds. J.Phys.Chem., 72: 3251-3260.

DEZELIC, G.J. and KRATOHVIL, J.P., 1960. Determination of size of small particles by light scattering. Experiments on Ludox colloidal silica. KOLLOID Z., 173: 38-48.

DUURSMA, E.G., 1974. The fluorescence of dissolved organic matter in the sea. In: Optical aspects of oceanography. Editors N.G. JERLOV and E. STEEMANN NIELSEN. Academic Press, London. 237-255.

EASTMAN, J.W., 1967. Quantitative spectrofluorimetry - the fluorescence quantum yield of quinine sulfate. Photochem. & Photobiol., 6: 55-72.

EISENBRANDT, J., 1954. Intensitätsvergleich von Ramaneffekt und Fluoreszenzstrahlung. Optik, 11: 557-561.

FARINATO, R.S., and ROWELL, R.L., 1976. New values of the light scattering depolarization and anisotropy of water. J.Chem.Phys., 65: 593-595.

FRY, E.S., 1974. Absolute calibration of a scatterance meter. In: Suspended solids in water. Edited by R.J. GIBBS. Plenum Press, New York. :101-109.

HARRISON, V.G.W., 1946. The light-diffusing properties of magnesium oxide. Phys.Soc.London, 58: 408-419.

HØJERSLEV, N., 1971. Tyndall and fluorescence measurements in Danish and Norwegian waters related to dynamical features. Rep. Inst. Phys. Oceanogr., Univ. Copenhagen. 16: 46 pp.

JERLOV, N.G., 1953. Particle distribution in the ocean. Rep. Swedish Deep-Sea Exped., 3: 73-97.

JERLOV, N.G., 1976. Marine optics. Elsevier Scient.Publ. Comp. Amsterdam. 231 pp.

KALLE, K., 1951. Meereskundlich-chemische Untersuchungen mit Hilfe des Pulfrich-Photometers von Zeiss. VII. Mitteilung. Die Mikrobestimmungen des Chlorophylls und der Eigenfluoreszenz der Meerwassers. Dtsch.Hydrogr.Z., 4: 92-96.

KALLE, K., 1963. Über das Verhalten und die Herkunft der in den Gewässern und in der Atmosphäre vorhandenen himmelblauen Fluoreszenz. Dtsch.Hydrogr.Z., 16: 153-166.

KULLENBERG, G. and NYGÅRD, K., 1971. Fluorescence measurements in the sea. Rep. Inst. Phys. Oceanogr., Univ. Copenhagen. 15.17 pp.

KÖNIG, W., 1928. Elektromagnetische Lichttheorie. In GEIGER, H. and SCHEEL, K.: Handbuch der Physik. Verlag J. Springer. Berlin. 20: 141-262.

LANDOLT-BÖRNSTEIN, 1962. Zahlenwerte und Funktionen. 6th ed. 2/8. Optische Konstanten. Springer-Verl. Berlin.

MELHUISH, W.H., 1960. A standard fluorescence spectrum for calibrating spectro-fluorophotometers. J.Phys.Chem., 64: 762-764.

MELHUISH, W.H., 1961. Quantum efficiencies of fluorescence of organic substances: Effect of solvent and concentration of the fluorescent solute. J.Phys.Chem., 65: 229-235.

MIDDLETON, W.E.K. and SANDERS, C.L., 1951. The absolute spectral diffuse reflectance of magnesium oxide. J.O.S.A., 41: 419-424.

MOREL, A., 1974. Optical properties of pure water and pure sea water. In: Optical aspects of oceanography. Editors N.G. JERLOV and E. STEEMANN NIELSEN. Academic Press, London. 1-24.

MURPHY, W.F. and BERNSTEIN, H.J., 1972. Raman spectra and an assignment of the vibrational stretching region of water. J.Phys. Chem., 76: 1147-1152.

PARKER, C.A., 1968. Photoluminescence of solutions. Elsevier Publ. Comp. Amsterdam. 544 pp.

PERRIN, F., 1929. La fluorescence des solutions. Ann. phys., 12: 169-275.

PIKE, E.R., POMEROY, W.R.M. and VAUGHAN, J.M., 1975. Measurement of Rayleigh ratio for several pure liquids using a laser and a monitored photon counting. J. Chem. Phys., 62: 3188-3192.

PRICE, J.M., KAIHARA, M. and HOWERTON, H.K., 1962. Influence of scattering on fluorescence spectra of dilute solutions obtained with the Aminco-Bowman Spectrophotofluorometer. Appl. Opt., 1: 521-533.

PRINGSHEIM, P. and VOGEL, M., 1946. Luminescence of liquids and solids and its practical application. Interscience Publishers, Inc. New York. 201 pp.

PRITCHARD, B.S. and ELLIOTT, W.G., 1960. Two instruments for atmospheric optics measurements. J.O.S.A., 50: 191-202.

RAYLEIGH, Lord, 1918. On the scattering of light by a cloud of similar particles of any shape and oriented at random. Phil.Mag. 35: 373-381.

TELLEX, P.A. and WALDRON, J.R., 1955. Reflectance of magnesium oxide. J.O.S.A., 45: 19-22.

TYLER, J.E., 1963. Design theory for a submersible scattering meter. Appl. Opt., 2: 245-248.

WEBER, G. and TEALE, F.W.J., 1957. Determination of the absolute quantum yield of fluorescent solutions. Trans. Far. Soc., 53: 646-655.

WESTON, R.E., Jr., 1962. Raman spectra of electrolyte solutions in light and heavy water. Spectrochim.Acta, 18: 1257-1277.

WORONKOFF, G.P. and POKROWSKI, G.J., 1923. Über die selektive Reflexion des Lichtes an diffus reflektierenden Körpern. Z.Physik, 20: 358-370.

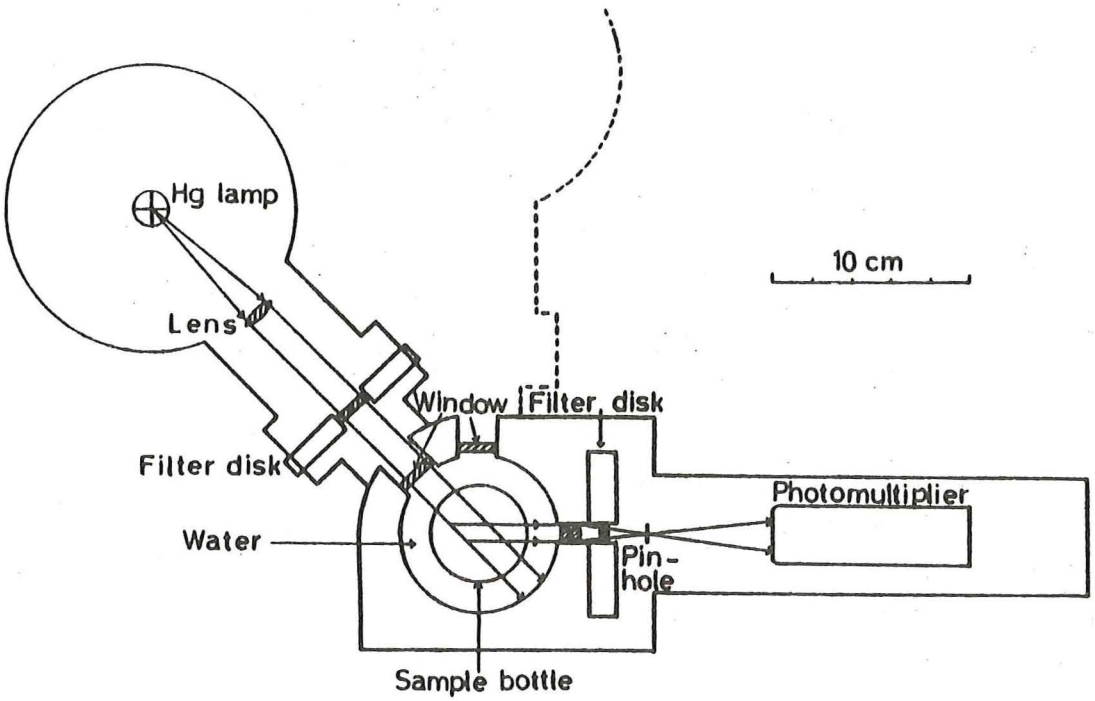

Fig. 1. The instrument

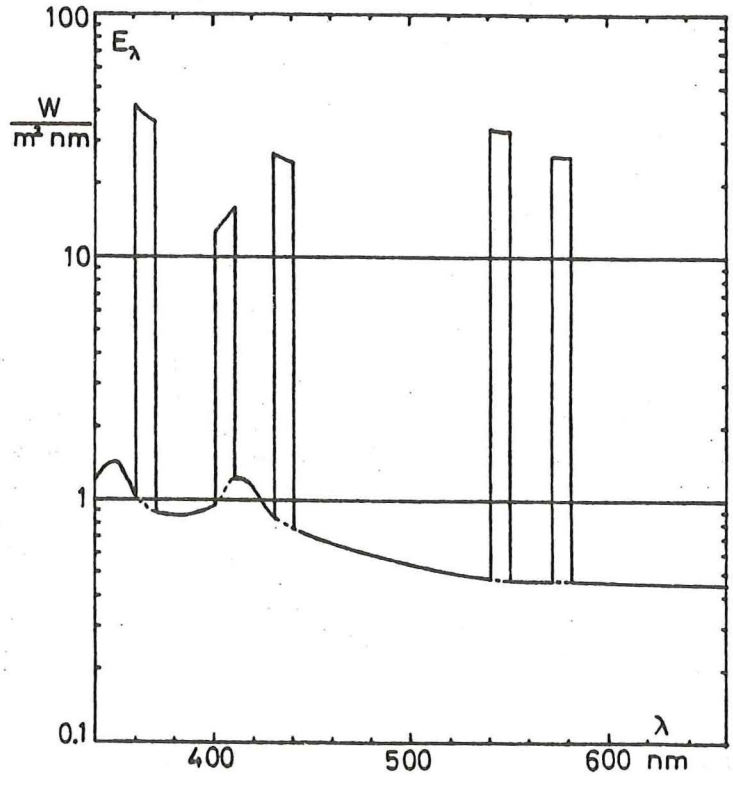

Fig. 2. Spectral irradiance distribution of the incident beam.

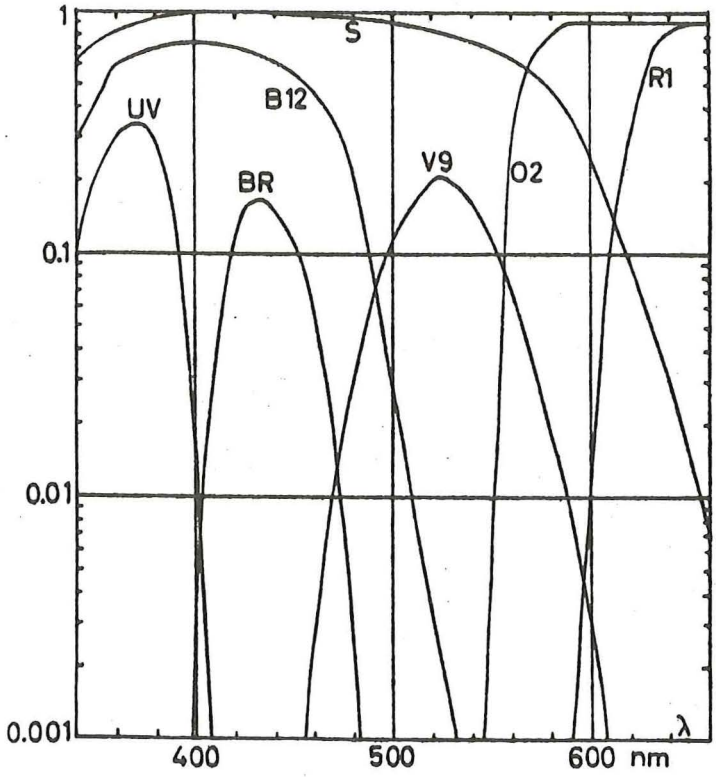

Fig. 3. Spectral sensitivity function S of the instrument in relative units, and the transmittances of the applied filters.

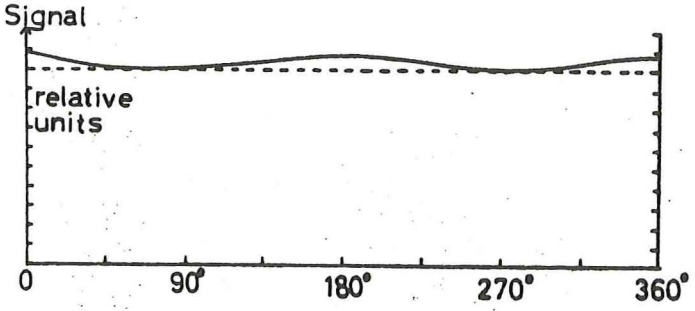

Fig. 4. The signal of the plexi-glass standard as a function of its angle of rotation.

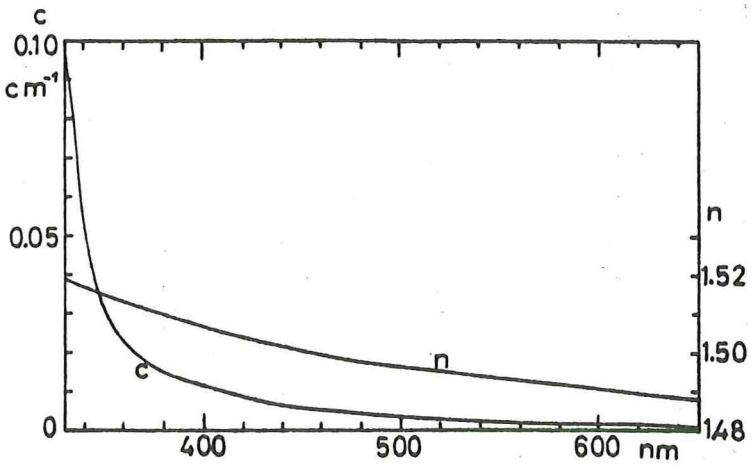

Fig. 5. The refractive index n (according to manufacturer) and the attenuation coefficient c of the standard.

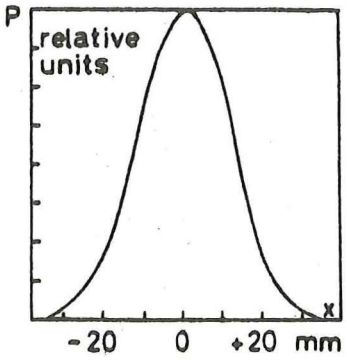

Fig. 6. The signal of the MgO disk as a function of its position in the sample section.

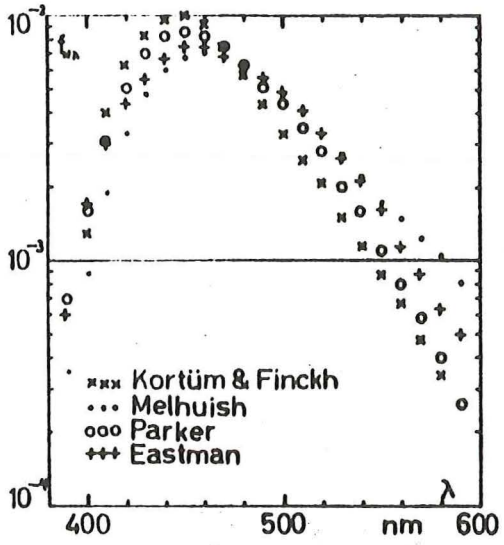

Fig. 7. The fluorescence spectrum $f_{N\lambda}(\lambda)$ of quinine bisulfate or quinine sulfate according to different authors.

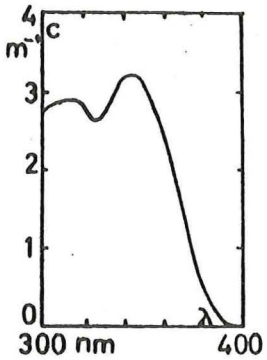

Fig. 8. The attenuation spectrum of 1 mg quinine sulfate in 1 litre of 0.01 N H_2SO_4.

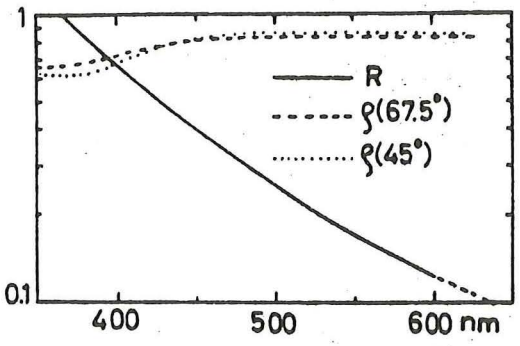

Fig. 9. The Rayleigh ratio R of water, normalized at 366 nm, and the reflectance ρ of tin in water.

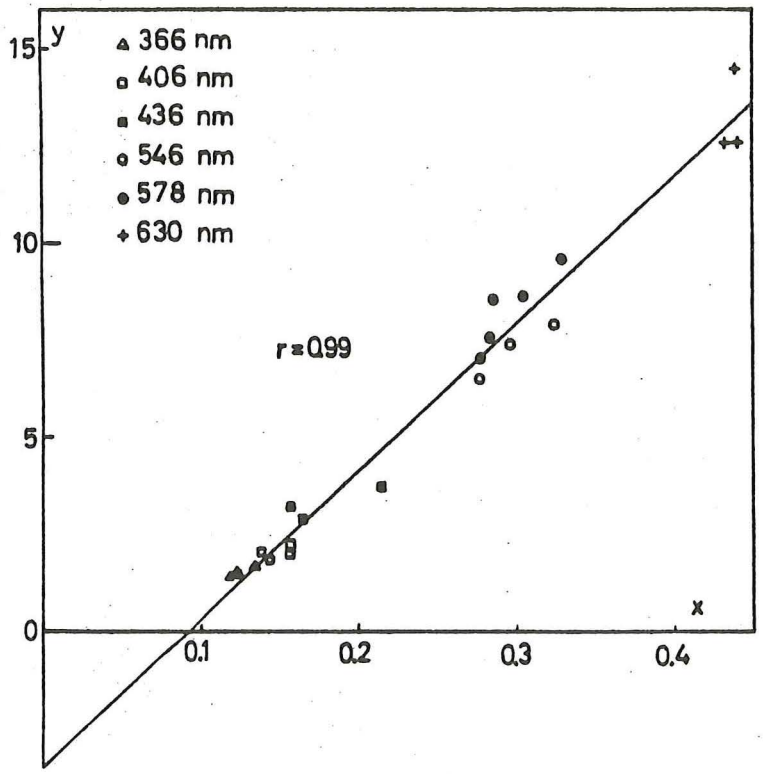

Fig. 10. For explanation see Chapter 4.4.3.

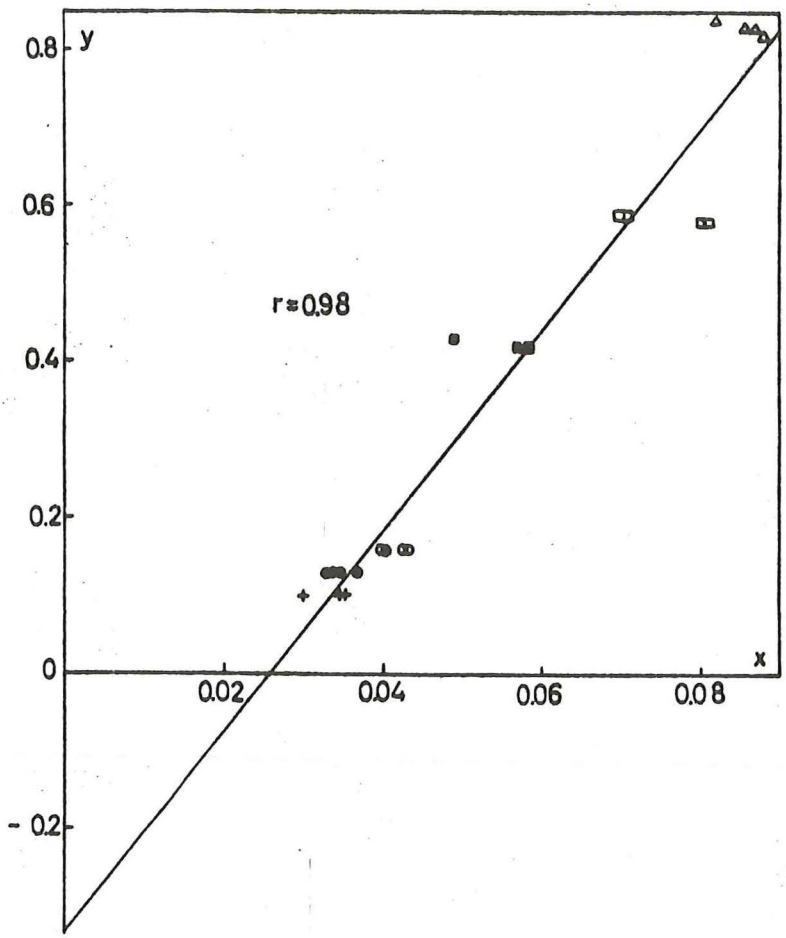

Fig. 11. For explanation see Chapter 4.5.1 and Fig. 10.

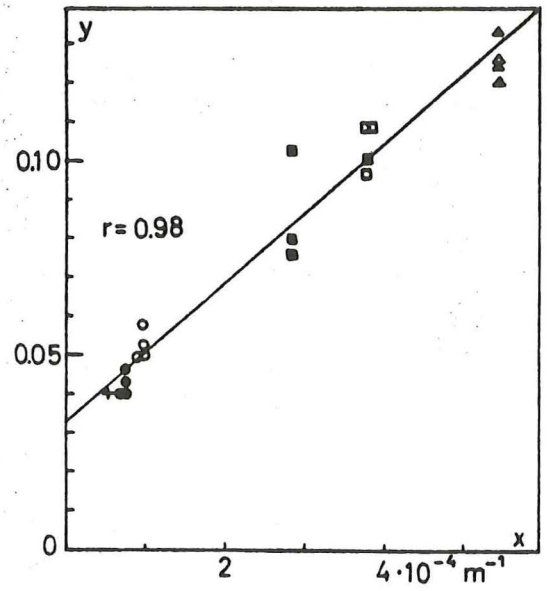

Fig. 12. For explanation see Chapter 4.6.1 and Fig. 10.

Fig. 13. (right) The scattering function $\beta_s(45^o,\lambda)$ of the plexi-glass standard

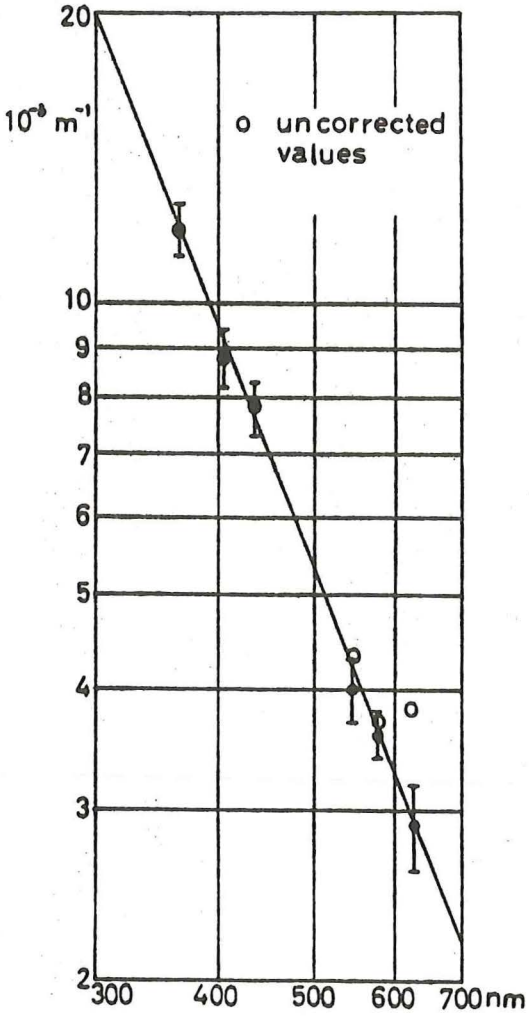

Fig. 14.(below) The Raman scatterance of water, scattered at 367 nm, in relative units according to MOREL. The hatched line is here assumed to be background fluorescence.

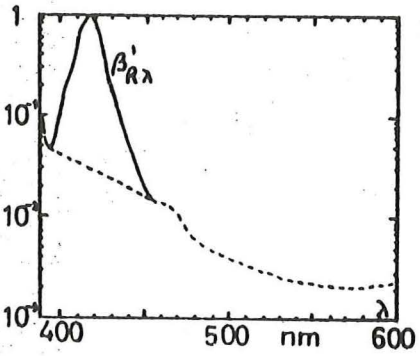

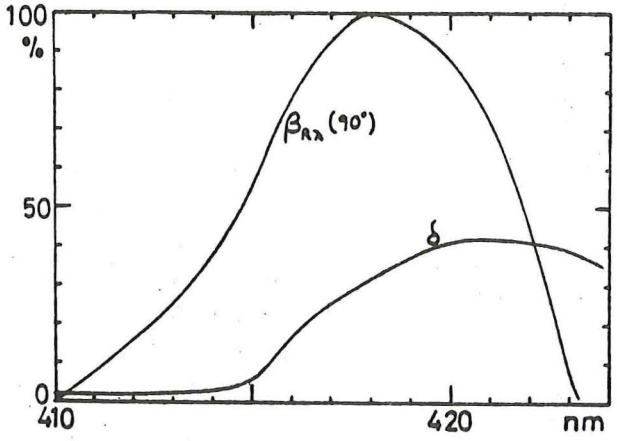

Fig. 15.(right) The Raman scatterance of water, $\beta_{R\lambda}$, in relative units, and the depolarization ratio δ, from data by CUNNINGHAM and LYONS (1973).